

Clinical Significance Of Creative 3D-Image Fusion Across【 CT+MR】 Modalities Based On Approach Of Characteristic Co-Registration

Matthew Jian-qiao PENG, Jing-Ming WU , XiangYang JU , Dao-Zhang CAI

Abstract— Since three-dimensional (3D) hybrid detector 【 CT+MR】 is not integrated well currently, this study aims to investigate a registration scheme for two-dimensional (2D) hybrid based on characteristic localization to achieve 3D-fusion from the images of CT and MR as a whole. A cubic oriented proposal of “9-point & 3-plane” for coregistration designs were verified to be geometrically practical. Human internal-feature points were sorted to combine with preselected external-feature points for matching process through 3D-reconstruction and virtual-dissection. By following the procedures of feature-extraction and image-mapping, the processes of “picking points to form plane” and “picking planes for segment” were executed. Ultimately, image-fusions were implemented at the real-time workstation Mimics based on auto-fuse techniques so called “information exchange” and “Signal Overlaying”. A complementary 3D-image across 【 CT+MR】 modalities, which simultaneously presents anatomic structures of hard-tissue and soft-tissue, was created with a detectable-rate of 70%, this is equivalent to detectable-rate of 【 PET+CT】 or 【 PET+MR】 with no statistically significant difference. Our approach of “9-point & 3-plane” offers a fresh idea for integration of digital imaging in mathematic consideration, and it facilitates a 3D vision that isn't functional yet for 2D hybrid imaging. This exploration is practical to those small hospital that are unable to afford expensive hybrid equipment.

Index Terms— Characteristic Registration, Hybrid Radiodetector, MRI, CT, PET, Image Segmentation, Cross-modality Image Fusion.

1 INTRODUCTION

SINCE its noninvasive detection of molecular metabolic information, Positron Emission Tomography (PET or PT) is used popularly in early diagnosis and accurate therapy, its anatomical visualization is however not clear due to its low resolution spatially, and thus is only considered as a detector for localization^[1] functionally. Magnetic Resonance Imaging (MR or MRI) shows superior contrast to soft-tissue^[2] but inferior to hard-tissue than Computed Tomography (CT) does. Consequently, an image fusion is essential to obtain complementary information in the area of diagnostics and treatment^[3]. An image fusion can be classified as Cross-Modality imaging (Images of diverse sources scanned on diverse detective system at duration apart) and Hybrid imaging (Images of diverse sources scanned on a single detective system simultaneously).

The hybrid imaging 【PET+CT】 product has been accepted popularly for 10 years commercially, however, the hybrid machine (two devices in one) of 【CT+MR】 product introduced to the clinic last year remains in two-dimensional (2D) phase as hardware-based^[4], whereas a hybrid detector with three-dimensional (3D) function has not been well integrated yet, it should be realized better by the path of “Image Fusion” alternatively, it is doubtlessly a critical issue of diagnostics in radiology and is representing a novel direction for development of nuclear imaging. Based on our previous accomplishment of researching image fusion in multimodalities of 【PET+CT+MR】^[5], we are analyzing 【CT+MR】 fusion in further by concreting “9-point & 3-plane” principle in this paper.

2 MATERIALS AND METHODS

2.1 Research Target

Twenty samples were extracted from the “Table of Random Number,” which were drawn from 200 patients who were enrolled in our hospital and primarily suffered by cancers during 2010 to 2012. The sample group included 6 females plus 14 males aged from 21 to 80 (mean, 60.5±15.4) years. The three cases selected by this article with significant aspect of image fusion are: case #00321246, female, 54 years old, suffered from Right side breast cancer; case #00333803, male, 63 years old, suffered from Left side lung cancer; case # 00317106, male, 59 years old, suffered from Left side lung cancer; case #00316561, male, 38 years old, suffered from Central type carcinoma of right lung; case #00331963, female, 68 years old, suffered from double gout of arthritis (informed consents were obtained from all patients).

2.2 Instrumental Equipment

MRI of “Intera1.5T, Nova Phillips Healthcare” made in Netherland; “Aquilion TSX-101A” CT made in Toshiba Japan; and the Medical Imaging Software used is “Mimics-14” Materialise made in Belgium.

- *Dr. Matthew J. PENG is a Senior Medical Engineer of Guangdong Orthopedic Institute @ Southern Medical University. His current research is regarding image processing coupled with computational diagnostic in Orthopedic, China; Email: 18922346634@163.com*
- *Dr. Jing-Ming WU, Chief Resident in Spinal Surgery at 1st Affiliated Hospital of Guangzhou Medical University, his research interests is Orthopedic implantation. Email: drwujm@163.com*
- *Dr. XiangYang JU is the Head of Image Processing Group, Medical Devices Unit, Department of Clinical Physics and Bioengineering, University of Glasgow, U.K. Email: x.ju@dental.gla.ac.uk*
- *Corresponding Author: Professor Dao-Zhang CAI is a Chief Resident in Joint Surgery, Vice president of 3rd Affiliated Hospital @ Southern Medical University, China. Email: daozhang@medmail.com*

2.3 Proposed Method

2.3.1 Somatotopic localization

A Fast-holder was placed on the patient’s feet by plastics Vacuum-Human-Cushion and the patient’s head was fixed with dedicate loops to keep the same exposure and to minimize physical position errors during the [MR] and [CT] examinations undertaken in different durations^[4]. The position-line is localized usually by selecting four points: from a patient’s middle submaxillary, supraorbital foramen and entrecejo; and three points: from a patient’s nipples and sternal angle. These points are marked by small “Lead Capsules” as fluorescence symbols before scanning, and these remarkable somatotopic localizations are able to not only suggest the approximate region of examination but also provide reference to locate coregistration points of the next step after images established.

2.3.2 Data acquisition

2.3.2.1 CT scan protocol

The CT imaging parameters are as follows: Slice thickness = 0.6 mm, Voltage = 120kV, Interval gap = 5 mm, Intelligent auto current = 50 mA/s ~ 150 mA/s, Field Of View (FOV) = 350 x 350 mm², and Pitch = 1.0. All patients were undertaken by supine position with arms up from parietal bone to hip joint to capture axial images, while coronal and sagittal were acquitted by multi-plane reformation (MPR)^[3,6].

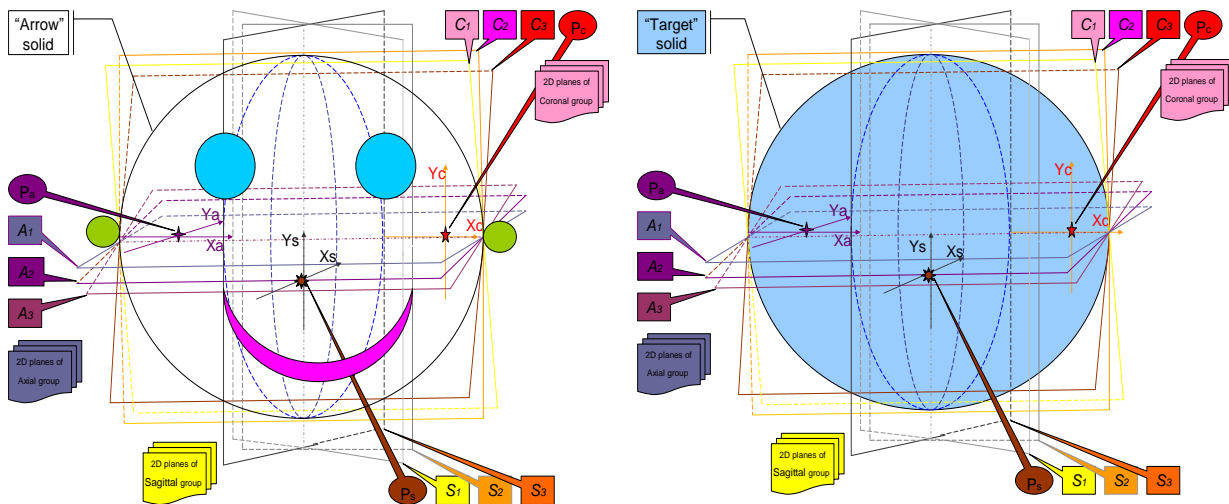
2.3.2.2 MR scan protocol

The MR imaging parameter are as follows: Slice thickness = 2 mm, Repetition Time (TR) = 500 ms, T1-weighted Turbo Spin-Echo (TSE) sequence without interval, Echo Time (TE) = 17 ms, Number of Signals Acquired (NSA) = 3, pixel size = 0.98 x 0.98 x 1.10 mm³, Flip angle = 90°, Matrix = 256 x 256, and Field Of View (FOV) = 300 x 240 mm². Data acquisition mode is similar as the standard as idem #2.3.2.1.

2.3.3 Experimental procedure

2.3.3.1 2D co-registration

The raw data collected from [MR] and [CT] in Digital Imaging and Communications in Medicine (DICOM) were input onto Mimics-14 workstation. These sources of image from diverse devices were transferred, exchanged and then constructed to be initial 3D of single modality ([CT] “arrow” solid or [MR] “target” solid). A method of “9-point & 3-plane” coregistration composed of 2 steps was implemented (as sketched by Plot 1): <1> “3-plane” principle: in the 3D image of “arrow” solid, 3 “extra characteristic (feature) points” (axial point called Pa, sagittal point called Ps, and coronal point called Pc) are picked according to special human structures (bone landmark as the first choice). Among the 3 groups of the transverse plans (axial group composed of A1, A2 & A3; coronal group composed of C1, C2 & C3; and sagittal group composed of S1, S2 & S3), which pass through each of those characteristic points (Pa, Pc, Ps), by the way of selection and virtual segmentation, 3 characteristic planes in 2D are extracted totally as follows in turn: an axial plane A3 from the 1st plane group, a coronal plane C2 from the 2nd plane group, and a sagittal plane S3 from the 3rd group. In the 3D image of “target” solid, similarly, three 2D “thin planes” of axial, coronal and sagittal are selected and virtually cut away. <2> “9-point” principle: with reference to the concrete process of item #4.1, We also built 3 “mixed feature points” (i.e., PB2+ PB3+PB4) upon each “feature plane” (i.e., S3), specifically, starting from 3 x 3 = 9 “focus points” in a series, these 3 segmented planes (i.e., plane A3, plane C2 or plane S3) scanned from this “Arrow solid” radio detector and those 3 planes (says plane A3, plane C2 or plane S3) scanned from that “Target solid” detector are doubly aligned to be coincided set by set^[7] (as sketched by Plot 2) correspondingly.



Plot 1: Co-registration method of “3-plane” sketched inside cartoon head

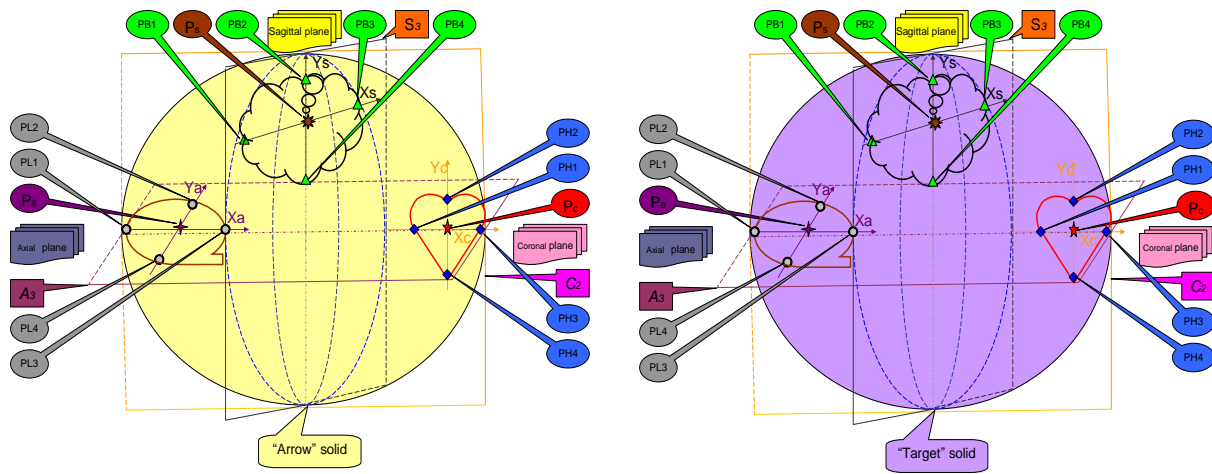
2.3.3.2 2D image fusion

Based on the cubic registration^[8] of “3-plane & 9-point” rule mentioning above, similarly, [MR] images are mapped associatively to [CT] images. By following the interface of Mimics-14 graphics toolkit upon oriented image, the selection

of merging is performed. There are twelve methods optionally for image signal to overlay, such as “maximize / minimize / average / plus / subtract / multiply / divide / differentiate”, according to clinical needs of “earlier findings” for this pilot study, we prefer “plus” based on signals yielded but regardless

of tissue sources, an algorithm similar to the superposition principle of “value composition” when “sine” (or “cosine”) waves of various wavelength (or frequency) meet together acoustically, mathematically, or optically to amplify any

abnormal tiny signals earlier found]. Then, all images are combined by following the Auto-Fusing style of information exchanged by the Signal Overlaid technique (“composition value” is visualized immediately).



Plot 2: Co-registration method of “9-point” sketched inside cartoon organs

2.3.3.3 3D re-construction

After the 2D images merged by step #2.3.3.2 are imported onto Reversal Soft called Mimics, point cloud mesh and triangulated grids are then exported, and then edited by the ways of compressing, fairing, padding and erasing on real-time workstation. Computer Aided Design (CAD) models are then organized by execution of Boolean. The curved surfaces of outside or inside in “Non-Uniform Rational B-Splines (NURBS)” are then re-drawn, and these multiple surfaces are then “sewn” into 3D solid model. The procedure of #2.3.3.2, #2.3.3.3 can be reversed in parallel specifically as: process #2.3.3.3 first to reconstruct 3D[CT] & 3D[MR], and then by reference of #2.3.3.2. Eventually, these 2 cubic solids were merged into 3D[CT+MR].

2.3.4 Data analysis

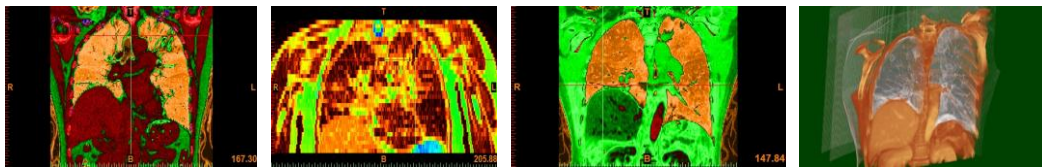
By using the methodology of “Double Blind” (each reads image without communication individual, with clinical information erased), the visualization efficiency of CT/MR/ PET as well as their inter-merging images for these 20 cases experiment were analyzed. A 5-expert team was formed by selecting specialists with similar qualification and proficiency, which includes 3 radiologist and 2 nuclear medicine physician. Every expert evaluated each image by considering one judgment from the following 5 choices “Definite positive (+), Definite negative (-), Probable positive (+), Probable negative (±), and Non-recognition (x)”. In term of authenticity characteristic indications, such as “Sensibility, Specificity & Precision (Correctness)”^[9], since the imaging principle for these 3 devices are different, and body parts such as “head, knee, chest and abdominal” contains different tissues (hard or soft), and equipments such as CT/PET addressing various clinical needs to regularly provide information for variant experimental samples emphasizing tendency of different structures or metabolism, the specificities that image fusion uses to examine diseases are also different and become difficult to compare. Meanwhile, a patient is usually glad to accept gold-standard biopsy proven^[10] only when his/her radiologic diagnosis is “Positive (+)”. For those patients with “Negative

(-)” diagnosis, further section information is hard to collect, objective diagnostics of “Correct diagnostic indices” are thus difficult to acquire and can be ignored here. Therefore, our plan for experimental testing is limited to reliability index of rough census (labeled as “Absolute”, “Probable” & “Indistinguishable”) until visualization index reaches “uniformity”.

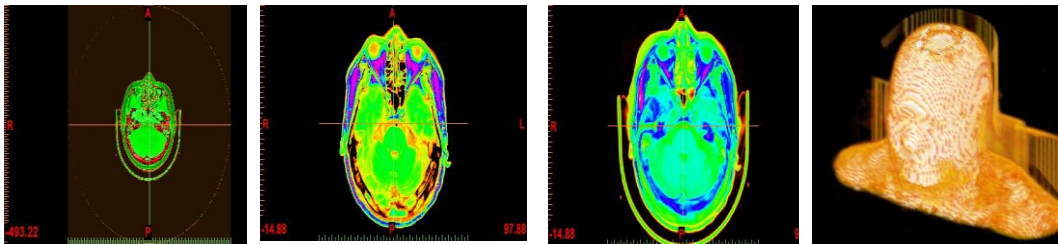
3 COMPARATIVE RESULTS

3.1 Imaging Effect

According to the feature of each imaging system, [MR] provides superior soft-tissue contrast but inferior hard-tissue contrast, whereas [CT] provides superior hard-tissue contrast but inferior soft-tissue contrast. As a specific example of resident account #00321246, bright hard-tissue from [CT] is illustrated in Fig 1A, clear soft-tissue from [MR] is illustrated in Fig 1B, the comprehensive dual images [MR+CT] such as Fig 1C & 1D compose signal properties from both soft-tissue and hard-tissue, and thus able to deeply acquire their correlation among pathologic tissues and organs^[6]. For more specific instances of resident account #00317106 & #00331963, the advantages of [CT+MR] taken from both [CT] and [MR] are expressed by Fig 2 & Fig 3.



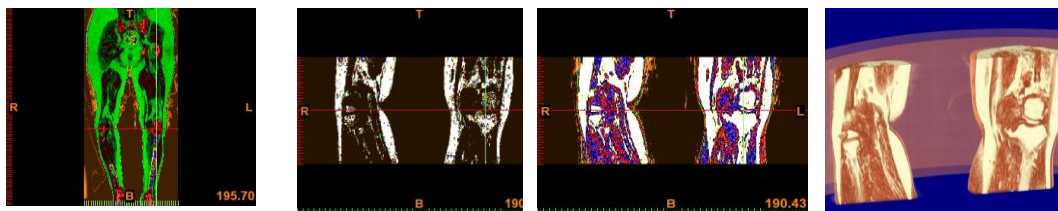
1A: CT coronal 1B: MR coronal 1C: [CT+MR] coronal 1D: [CT+MR] 3D
Fig 1: CT as arrow image, MR as target image, chest 2D→3D [CT+MR] cross modalities fusion



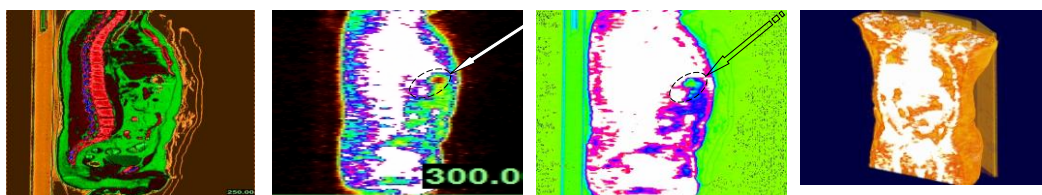
2A: CT axial 2B: MR axial 2C: [CT+MR] axial 2D: [CT+MR] 3D
Fig 2: [CT] as target image, [PET] as arrow image, head 2D→3D [CT+MR] cross modalities fusion

In order to meet the statistics need of further comparison, we considered an additional image fusion. Based on the strength of each imaging system, [CT] presents higher contrast in morphology for hard-tissue however lacks functional information, as shown in Fig 4A, illustrating density lesion with nature unknown, whereas [PET] diagnoses minimal pleural abnormality clearly but is poor in addressing region, as Fig 4B illustrates. By then, the image of fused [PET+CT] delivers more accurate and convenient basis for radiologist to interpret radiographs than individual [CT] or individual

[PET], respectively. For instance of resident account #00316561, half-distinct images created from conventional [CT+PET] present the vicinity of structures and metabolic activities simultaneously, such as Fig 4C & 4D, not only define the location of cancer lesion found out by [CT]^[10] but also depict the nature of lung tumor by [PET], “Central carcinoma at right lung” was thus discovered in time initially for this case^[11] as a result, because metabolic changes occur prior to morphologic structures.



3A: CT coronal 3B: MR coronal 3C: [CT+MR] coronal 3D: [CT+MR] 3D Cut
Fig 3: CT as arrow image, MR as target image, knee 2D→3D [CT+MR] cross modalities fusion



4A: CT sagittal 4B: PET sagittal 4C: [PET+CT] sagittal 4D: [PET+CT] 3D

Fig 4: PET as arrow image, CT as target image, body 2D→3D [PET+CT] cross modalities fusion

In order to meet the statistical need for comparative study, we investigated an extra image fusion as follows. Based on the strength of each imaging system, [MR] visualizes higher resolution in morphology for soft-tissue but lacks definitively functional information, whereas [PET] provides functional information in metabolism but is limited on anatomic

visualization. As a specific example of resident account #00333803, [PET] demonstrates a metabolic lesion of compact opacity in the lung with position unspecified as Fig 5A illustrates, [MR] shows high contrast for parenchyma but low sensitivity in tumor sign as Fig 5B illustrates, while images of [PET+MR] combination express complementary

diagnostic information in structure and metabolism as

illustrated by Fig 5C & 5D

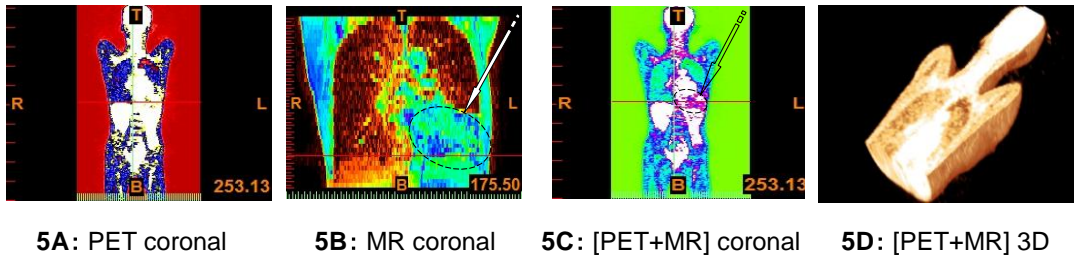


Fig 5: PET as arrow, MR as target image, chest 2D to 3D [PET+MR] cross modalities fusion

3.2 Visualization Evaluation

By following the above method of #2.3.4, the effect of each of the 20 images were “graded” professionally by our 5-expert team and thus cumulated 20 x 5 = 100 items of “score”. The result of this survey is listed in table 1.1. If the

distinguishable-degree is classified into 3 bigger groups, such as: “Probable positive + Probable negative” = “Probable (+)”, “Definite positive + Definite negative” = “Absolute (+)”, “Non-recognition (x)” = “Indistinguishable (x)”, this table is simplified and is added up to form table 1.2.

TABLE 1.1 EVALUATION ON RESOLUTION OF MULTIMODALITY IMAGE IDENTIFICATION

Source	[CT+MR]	[PET+MR]	[PET+CT]
(+)	59	49	46
(+)	11	17	14
(-)	11	7	8
(⊖)	9	13	16
(x)	10	14	16
Total	100	100	100

TABLE 1.2 CLASSIFICATION OF DUAL-MODALITY IMAGE IDENTIFICATION

Source	[CT+MR]	[PET+MR]	[PET+CT]
(x)	10	14	16
(⊖)	20	30	30
(+)	70	56	54
detectable (%)	70	56	54

The outcome of this survey is analyzed by SPSS-16.0 and expressed as the cylinder-curve and broken-curve in Fig 6. Based on “Fridman Testing” of multiple-samples matched-pair, P=0.027<0.05 indicates a “significant difference” for discrimination of fusion result between single modality and multimodality. Therefore, for the dual modalities in Fig 6, the

comparisons of 2 vs 2 are further urgent such as: [PET+MR] : [PET+CT] and [PET+MR] : [CT+MR]. The 2 “P-values” are found to be greater than inspective level. In consensus, all matched-pairs result in “no significant difference” [7] as demonstrated in the other tables (table 1.0, table 2.0, table 2.1 and table 2.2).

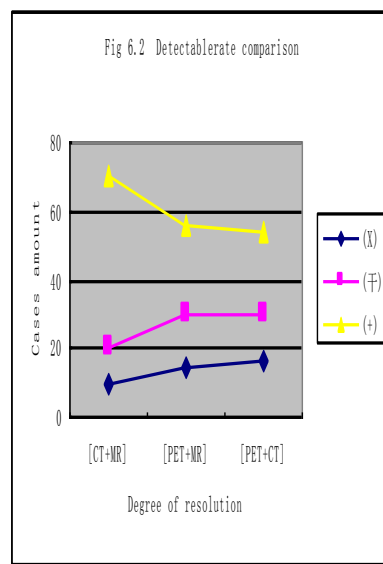
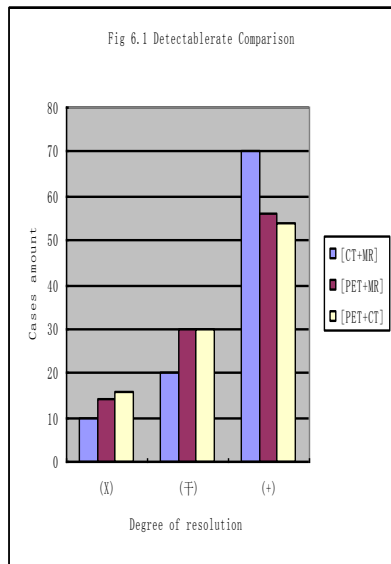


Fig 6: Comparison of contrast single vs dual modality

TABLE 1.0 RANKS

	Mean Rank
CT+MR	2.16
PET+MR	1.95
PET+CT	1.89
Test Statisticsa	
	100
Chi-Square	7.243
df	2
Asymp. Sig.	.027

K-related test

TABLE 2.0 TEST STATISTICS OF EACH PARTNERSHIP

Test Statistics ^b		Test Statistics ^b		
		【 PET+CT】 vs 【 PET+MR】	【 PET+MR】 vs 【 CT+MR】	
Z		-401a	Z	-1.921a
Asymp. Sig. (2-tailed)		.688	Asymp. Sig. (2-tailed)	.055
a. Based on positive ranks.		b. Wilcoxon Signed Ranks Test		

TABLE 2.1 PARTNERSHIP TESTING OF 【 PET+MR】 V.S. 【 PET+CT】
【 PET+MR】 vs 【 PET+CT】 Crosstabulation

		【 PET+CT】			Total
		(X)	(+)	(+)	
【 PET+MR】	(X) Count (% within)	3 (21.4%)	4 (28.6%)	7 (50.0%)	14 (100.0%)
	(+) Count (% within)	5 (16.7%)	13 (43.3%)	12 (40.0%)	30 (100.0%)
	(+) Count (% within)	8 (14.3%)	13 (23.2%)	35 (62.5%)	56 (100.0%)
Total	Count (% within)	16 (16.0%)	30 (30.0%)	54 (54.0%)	100 (100.0%)

z=0.401, p=0.688 > (Inspection level =0.05/2=0.025)

TABLE 2.2 PARTNERSHIP TESTING OF【 PET+MR】 V.S. 【 CT+MR】
【 PET+MR】 vs 【 CT+MR】 Crosstabulation

		【 PET+MR】			Total
		(X)	(+)	(+)	
【 CT+MR】	(X) Count	3	3	4	10
	% within 【 CT+MR】	30.0%	30.0%	40.0%	100.0%
	(+) Count	2	8	10	20
	% within 【 CT+MR】	10.0%	40.0%	50.0%	100.0%
Total	(+) Count	9	19	42	70
	% within 【 CT+MR】	12.9%	27.1%	60.0%	100.0%
	Count	14	30	56	100
	% within 【 CT+MR】	14.0%	30.0%	56.0%	100.0%

z= -1.921a, p= 0.055 > (Inspection level =0.05/2=0.025)

4 DISCUSSION

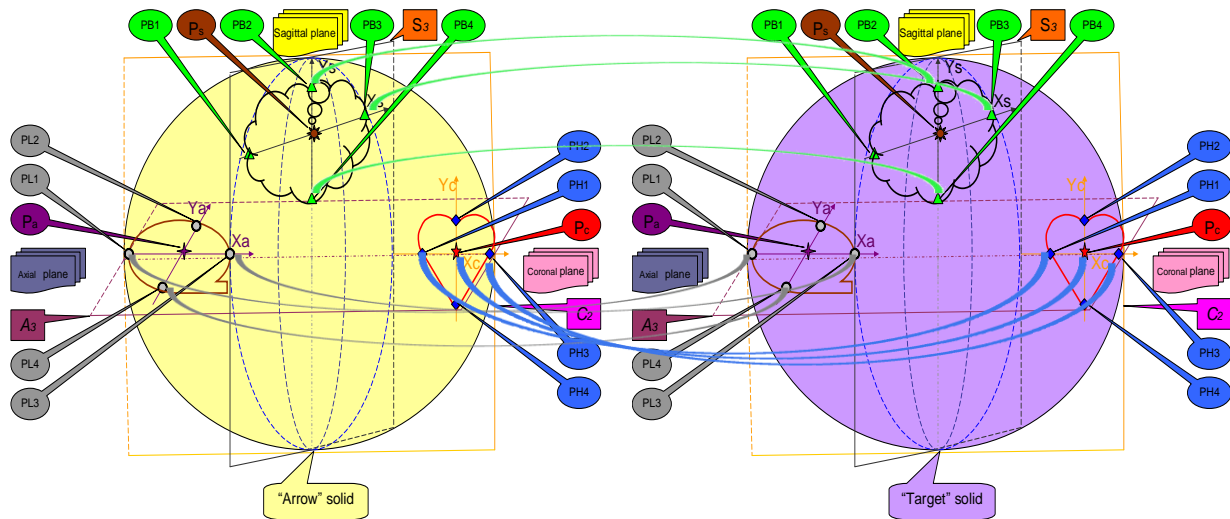
4.1 Mechanism for Coregistration Fusion

Brown LG et al summarized in 1992 a so called 2-step procedure^[8] for "Image exchange" and "Image locating": <1> "Image exchange" ensures that each voxel / pixel represents equal size of spatial area practically by scenarios of rotation translation, reflection, and so on. <2> In term of "Image locating", two methods like "internal characteristic based" (primarily based on configuration and segmentation) and "external characteristic based" are carried out in this research. Following the procedure of "Feature extraction" and "Image mapping" (such as "Arrow" PB2 linking "Target" PB2, similarly in turn: "Arrow" PB3 vs "Target" PB3, "Arrow" PB4 vs "Target" PB4, as sketched by Plot 3), and starting from marking and dividing internal features (tissue characterization), the process of "picking planes for segmentation" and "picking points to form planes" are fulfilled. The critical step and principal condition of image fusion is "Localizing registration", it enforces correlation so called "one to one" through which one floating image maps another spatially in relocatability^[3], so that certain anatomic point (of the human body) of the 1st image (intersection point

on "Arrow" Liver, PL1) correspondently locates on the same position as another point of the 2nd image (next PL1 on "Target" Liver) at the coordinate set ($\{X_a, Y_a\}$ relatively). Here is the process in detail (as also demonstrated by Plot 3): on the segmented planes where each human "feature point" locates, geometrically align its principal axis and center mass by rotation or translation. The double vertical axis of "Coordinate Set Like" (Coordinate $\{X_a, Y_a\}$ for axial plane, or, Coordinate $\{X_c, Y_c\}$ for coronal plane, or Coordinate $\{X_s, Y_s\}$ for saggital plane) are auto-created on these transactions (formed inside the domain where crossover structural lines of body surface, organ boundaries or infectious lesion are joined). These double-axis are extended until they intersect with the plane edge or organ (Liver called "L", Heart called "H", or Brain called "B") surface. As a result, there lies 4 intersect-points (internal "feature points") existing, such as: PL1 & PL3 (extracted by Liver intersecting X_a at axial plane), PL2 & PL4 (extracted by Liver intersecting Y_a similarly), in additional to the previous human external "feature points" (P_a at axial plane) where the previous plane passed through. There, 3 mixed (internal plus external) "focus points" (select PH1, PH3 & P_c extended by organ Heart) can then be picked from at least $(4+1=)$ 5 (PH1, PH2, PH3, PH4 & P_c) of them. By then, we totally have 3

feature planes (A3, S3 & C2) decided by 3 external feature points (Pa, Ps, & Pc), and we also picked 3 focus points from each of them as “registration points”. When the imaging workstation pre-judges that the coordinate transformation of (3×3) 9 focus points turn out to be minimal, the two 3D solids of “9 to 9 based” are catchable and entirely located (so called “locked”). For a geometrical example: suppose there is a registration point R(a,b,c) on plane M, and a correspondent registration point Q(i,j,k) on correspondent plane N, when $\sum=(a-i)^2+(b-j)^2+(c-k)^2$ is minimums, the square root of \sum (says $\sqrt{\sum}$) is also optimal; when these 2 points are superimposed, $\sum=0$ represents reduplication of R, Q. Obviously, the superiority of “9 points & 3-plane” algorithm on other

algorithms is committed by the scientific foundation of “3 planes forming a solid, 3 points forming a plane” principle geometrically in dedication. The level of accuracy for “Localizing registration” affects directly the quality of image fusion due to none-staple factors, such as the biological activities of their internal organs or physical repositioning as well as patients’ posture change. The situation that data gathered are incompatible will result in difficulties for co-registration followed-up. This is the disadvantage of this cross-modality fusing experiment, and it is difficult to overcome. By then, the degree of accuracy is only able to be handled by visual insight of the processor and his / her delineating experience



Plot 3: “Localizing registration” mapping “focus points” of solid “Arrow” vs “Target” sketched between cartoon organs

There are 2 solutions for image integrity: valuable information is extracted from “this” image to combine to “that” image; valuable information is alternately extracted from both images and then casted onto new imaging space^[4]. The first way is referenced for this paper: the image of “targeted” set is treated as image background called vector, the preferable image of “arrow” set is treated as a carrier for supplementary information, and its unmoral regions are to be extracted and casted onto the base image. After matching, the image fusion is constructed by 2 categories of solution: fusion of image-feature based^[3], and fusion of image-pixel based. Here, we pick the first one. In this experiment, “Overlap Technique” is chosen according to clinical need based on cubic registration. Among the 12 sorts of techniques of item # 2.3.3.2, overlapping is considered to be the majority that is feasible for enforcing fusion and thus more practical popularly.

4.2 Clinical Significance of Image Fusion

Image fusions are classified into variants of series as they are so diverse, suitable choices thus must be selected addressing to specification of different diseases besides common aspects. For lung tumor and mammary, either 【MR】 or 【CT】 or 【PET】 scan presents identical value^[11]. For secondary oncologic metastasis or lymphoma, the sensitivity and specificity of 【PET+CT】 fusion are higher and thus preferable, respectively. The potential indications in which 【PET+MR】 may be superior to 【PET+CT】 will be those in

which 【MR】 alone has been found more accurate than 【CT】 alone, including tumors of liver, musculoskeletal, intracranial, neck, breast and prostatic, for metastatic spread^[12,13]. The detectable rate of 【PET+MR】 is comparably higher and probably enhance the clinical assessment as a result. 【CT】 is considered to be a good choice when evaluating metal implants for their integrity and correct placement, rule out possible adjacent fractures and capable of quantifying intervertebral ossification processes, and is considered the diagnostic imaging modality of option to assess metal implants for incorrect placement or possible disruption, whereas the quality of soft tissue information is considered to be beyond 【MR】 standards. The assessment of metal structures such as spondylolysis material is almost impossible in 【MR】 due to serious susceptibility artifacts. However, 【MR】 provides important soft tissue information about possible intervertebral disc pathologies, condition of the spinal cord, compression of spinal nerve roots, presence of adjacent degeneration to the metal implants such as disc degeneration caused by a misplaced screw. Therefore, combination of both modalities on one image 【MR+CT】 could yield the ability of diagnosing multiple findings such as disc degeneration adjacent to fused segments (【MR】 information) and misplaced screws (【CT】 information) faster and more convincing. In musculoskeletal radiology, to combine the information about implants and bone provided by 【CT】 with the soft tissue information of 【MR】 imaging is practically

relevant; In orthopedics diagnostics, the position of metal implants of a lumbar spine could be assessed reliably on fused images; similarly, in cardiac radiology, image fusion is getting more important by combining [MR] information about myocardial perfusion and [CT] information about coronary artery disease. Moreover, the fusion of [MR+CT] data sets has been also employed in radiation therapy for better delineation of the desired target field and in craniofacial surgery in order to enhance computer-aided guidance during operation. In short, [CT+MR] image fusion is feasible, accurate, fast and easy to implement in daily routine work^[14-16].

5 CONCLUSION

This article introduces a co-registration scheme “9-point & 3-planes” for different modal sources [MR] & [CT] to be fused into an integrated image [CT+MR]. “Overlap” function on the imaging system called Mimics-14 is applied comprehensively to be the primary technique. This sort of combinative image structured from hard & soft tissue simultaneously can be faculties for early diagnostics by detecting new clues especially in craniofacial surgery or orthopedics. Wherein its efficiency is uncompetitive to hybrid [CT+MR] to be clinical routine tool adequately^[7,16], this exploration is practical to those small hospital that are unable to afford the above expensive hybrid equipment.

REFERENCES

- [1] Schulthess GK, Schlemmer H-PW. A look ahead: PET/MR versus PET/CT. *Eur J Nucl Med Mol Imaging* 2009; 36:S3–S9.
- [2] Ardekania BA., Guckemus S, Bachman A, et al. Quantitative comparison of algorithms for inter-subject registration of 3D volumetric brain MRI scans. *J. Neurosci. Methods* 2005; 142(1):67–76.
- [3] Karlo CA, Steurer-Dober I, Leonardi M, et al., J. MR/CT image fusion of the spine after spondylodesis: a feasibility study. *Eur Spine J* 2010. 19: 1771–1775.
- [4] Schlemmer H-P, Pichler BJ, Krieg R, et al. PET/MRI hybrid imaging: devices and initial results. *Eur Radiol* 2008; 18: 1077-1086.
- [5] Peng MJ, Ju X, Khambay BS, et al. Clinical significance of creative 3D-image fusion across multimodalities [PET+CT+MR] based on characteristic co-registration. *European Journal of Radiology* 2012, 81 (3): e406–e413.
- [6] Okane K, Ibaraki M, Toyoshima H, et al. 18F-FDG accumulation in atherosclerosis: use of CT and MR co-registration of thoracic and carotid arteries, *European Journal of Nuclear Medicine and Molecular Imaging*, 2006; 33: 590-594.
- [7] Schlemmer H-P, Pichler BJ, Krieg R, et al. An integrated MR/PET system: prospective applications. *Abdom Imaging* 2009; 34: 668–674.
- [8] Brown LG. A survey of image registration techniques. *ACM Computing Survey*, 1992; 24: 325-376.
- [9] Schulz V, Torres-Espallardo I, Renisch S, et al. Automatic three-segment MR-based attenuation correction for whole-body PET/MR data. *Eur J Nucl Med Mol Imaging* 2011; 38:138–152.
- [10] Nakamoto Y, Tamai K, Saga T, et al. Clinical value of image fusion from MR-PET in patients with head & neck cancer. *Mol Imaging Biol* 2009; 11: 46–53.
- [11] Heiss WD. The potential of PET/MR for brain imaging. *Eur J Nucl Med Mol Imaging*, 2009; 36: S105–S112.
- [12] Antoch G, Bockisch A. Combined PET/MRI: a new dimension in whole body oncology imaging? *Eur J Nucl Med Mol Imaging* 2009; 36: S113–S120.
- [13] Camara O, Delso G.; Colliot O, et al. Explicit incorporation of prior anatomical information into a nonrigid registration of thoracic and abdominal CT and 18-FDG whole-body emission PET images. *IEEE Trans. Med Imaging* 2007; 26: 164–178.
- [14] Brix G, Nekolla EA, Nosske D, et al. Risks and safety aspects related to PET/MR examinations. *Eur J Nucl Med Mol Imaging* 2009; 36: S131 – S138 .
- [15] Tahari AK, Bravo PE, Rahmim A, et al. Initial human experience with Rubidium-82 renal PET/CT imaging. *Journal of Medical Imaging and Radiation Oncology* 2014; 58: 25–31.
- [16] Giovanella L, Lucignani G. Hybrid versus fusion imaging: are we moving forward judiciously?. *Eur J Nucl Med Mol Imaging* 2010; 37: 973–979.

ACKNOWLEDGEMENT

This work is supported (No potential conflict of interest) by

1. GuangDong Dept. of Science Technology, China” granted project (#2011B050400029) titled: « Creative Thermal Simulation based on 3D Thermography» ;
2. GuangDong Natural Science Foundation, China” granted project (#S2011010005011) titled: « Creative Thermal Simulation based on 4D Virtual Thoracic Operation» ;
3. GuangZhou Dept. of Science Technology, China” granted project (#11S72020062) titled: « Operative Model of Thermal Simulation in Gynaecology based on 3D Thermography» ;
4. Guangzhou Dept. of Educational Research, China” granted project (#2012C005) titled: « Thermal Simulation in Orthopedics based on 3D Thermography» .